Absence of nematic order in the pressure-induced intermediate phase of the iron-based superconductor $Ba_{0.85}K_{0.15}Fe_2As_2$

Yan Zheng,[1] Pok Man Tam,[1] Jianqiang Hou,[1] Anna E. Böhmer,[2,3] Thomas Wolf,[2] Christoph Meingast,[2] and Rolf Lortz[1,*]

[1]*Department of Physics, The Hong Kong University of Science and Technology, Clear Water Bay, Kowloon, Hong Kong, China*

[2]*Institute for Solid State Physics, Karlsruhe Institute of Technology, P.O. Box 3640, 76021 Karlsruhe, Germany*

[3]*Fakultät für Physik, Karlsruhe Institute of Technology, 76131 Karlsruhe, Germany*

(Received 7 July 2015; revised manuscript received 17 February 2016; published 14 March 2016)

The hole doped Fe-based superconductors $Ba_{1-x}A_xFe_2As_2$ (where A = Na or K) show a particularly rich phase diagram. It was observed that an intermediate reentrant tetragonal phase, in which the C_4 fourfold rotational symmetry is restored, forms within the orthorhombic antiferromagnetically ordered stripe-type spin density wave state above the superconducting transition [S. Avci *et al.*, Nat. Commun. **5**, 3845 (2014); A. E. Böhmer *et al.*, Nat. Commun. **6**, 7911 (2015)]. A similar intermediate phase was reported to appear if pressure is applied to underdoped $Ba_{1-x}K_xFe_2As_2$ [E. Hassinger *et al.*, Phys. Rev. B **86**, 140502(R) (2012)]. Here we report data of the electric resistivity, Hall effect, specific heat, and the thermoelectric Nernst and Seebeck coefficients measured on a $Ba_{0.85}K_{0.15}Fe_2As_2$ single crystal under pressure up to 5.5 GPa. The data reveal a coexistence of the intermediate phase with filamentary superconductivity. The Nernst coefficient shows a large signature of nematic order that coincides with the stripe-type spin density wave state up to optimal pressure. In the pressure-induced intermediate phase the nematic order is removed, thus confirming that its nature is a reentrant tetragonal phase.

DOI: 10.1103/PhysRevB.93.104516

I. INTRODUCTION

Applying external hydrostatic pressure to the $AEFe_2As_2$ ("122") (AE = Ba,Sr,Ca) family of iron-based superconductors [1–8] has a similar effect as chemical ion substitution [9–18]. It serves as a control parameter which suppresses the static magnetic order of the parent compound and induces superconductivity. Electron doping can be achieved, e.g., by substitution of Fe^{2+} by Co^{3+} [9,10], while hole doping occurs upon substitution of Ba^{2+} by K^+ [11,12] or Na^+ [13]. In addition, isovalent doping is achieved by chemical substitution with isovalent ions of different size. The latter can be regarded as applying internal chemical pressure, which is, for example, achieved through substitution of As by P [14,15]. Pressure is regarded generally as a particularly clean way of tuning materials since only one sample is used for the study of a particular region of the phase diagram, which normally helps to minimize reducing the effect of crystalline disorder [8,19]. The normal state of the 122 materials is characterized by both a nematic order that reduces the rotational symmetry of the high-temperature tetragonal structure of C_4 symmetry to an orthorhombic twofold C_2 symmetry, and a spin density wave (SDW) order that causes a stripe-type antiferromagnetic spin arrangement in the FeAs layers [20]. There is growing evidence that the nematic order is an electronically driven instability, but it remains unclear whether it is primarily the result of orbital order or spin driven order [21]. Upon doping the parent compound, e.g., $BaFe_2As_2$, the nematic and SDW ordering temperatures are gradually suppressed, and superconductivity appears with the maximum transition temperature T_c close to the concentration where the structural and magnetic transitions are suppressed to zero [20].

In hole-doped 122 compounds such as $Ba_{1-x}K_xFe_2As_2$ and $Ba_{1-x}Na_xFe_2As_2$, the phase diagram appears to be particularly rich. In $Ba_{1-x}K_xFe_2As_2$, a new phase under pressure has been observed in resistivity measurements in the underdoped range with $x = 0.16$–0.19 [22], which appears within the magnetically ordered state. For example, only a small increase of T_c from 10 K up to ~17 K was observed when pressure was applied to a sample with $x = 0.16$ up to 1.25 GPa. For higher pressure, T_c decreased slightly and then saturated at ~15 K up to at least 2.4 GPa. A second, steplike resistivity drop occurred above T_c, with its onset increasing to almost 40 K for pressure of 2.4 GPa. More recently, it was shown that such an intermediate phase also appears at ambient pressure in a narrow doping range between ~24% and 28% of K substitution, and was associated with a reentrant tetragonal phase [23]. A similar ambient-pressure reentrant C_4 phase was previously observed in $Ba_{1-x}Na_xFe_2As_2$ [24]. This phase is associated with a spin reorientation that restores the C_4 rotational symmetry [24,25], and has been interpreted as an itinerant double-Q spin density wave state [26]. It is still unclear whether the force driving this transition is due to magnetic interactions, or the orbital reconstruction of the iron 3d states [24]. The pressure-induced intermediate phase in $Ba_{1-x}K_xFe_2As_2$ [22] and the reentrant C_4 phase at ambient pressure [23] are likely of similar origin, and additional data of other physical quantities would be highly desirable to confirm this.

In this paper we investigate the pressure phase diagram of a high-quality [23] single crystal of $Ba_{0.85}K_{0.15}Fe_2As_2$ with a variety of experimental probes, including resistivity, Hall effect, specific heat, and the thermoelectric Nernst and Seebeck coefficients, which we measure under pressure up to 5.5 GPa in a Bridgman-type pressure cell. This allows us to study the characteristics of the pressure-induced intermediate phase with a multitude of techniques that are rarely carried out under pressure, and to extend the phase diagram up to higher pressure to reveal the entire pressure range of the intermediate phase. In particular, the Nernst effect shows a strong sensitivity for the nematic order that coincides with the stripe-type SDW order up to optimal pressure. This nematic order is suppressed

*Corresponding author: lortz@ust.hk

in the intermediate phase, which confirms that the rotational C_4 symmetry is restored analogous to the reentrant tetragonal phase at ambient pressure.

II. EXPERIMENTAL DETAILS

The $Ba_{0.85}K_{0.15}Fe_2As_2$ single crystal was grown from self-flux in an Al_2O_3 crucible. Ba and K were mixed with prereacted FeAs in the desired ratio and filled into the crucible. The crucible was sealed in a steel container and heated to 1151 °C. Subsequently, the crucible was cooled very slowly to 1051 °C at 0.2–0.5 °C/h. At the end of the growth process the crucible was tilted and slowly pulled out of the furnace to decant the remaining flux. The exact K content x of the samples, which typically differs from the starting stoichiometry, was determined by energy-dispersive x-ray analysis (EDX) and by four-circle x-ray diffraction.

The high-pressure experiment was conducted in a modified Bridgman pressure cell in a pyrophillite gasket mounted on a tungsten carbide anvil with 3.5 mm active diameter [8,19]. As pressure medium, the soft "soapstone" steatite was used. Although it only offers quasihydrostatic conditions, its use is essential because of its low thermal conductivity, which enables us to thermally isolate the samples from the anvils during the specific heat and thermoelectrical measurements. At temperatures exceeding 10 K this is difficult with most common liquid pressure media. The drawback is that our samples are exposed to some pressure gradients, which are known to have a rather strong impact on the phase diagram of Ba122 [6,7]. Pressure gradients can strongly alter the phase diagram of Fe-based superconductors in the vicinity of structural phase transitions [6,7]. The applied pressure was determined with the help of a thin piece of Pb foil, which served as a manometer by monitoring the pressure dependence of its superconducting critical temperature [27–30]. With special care taken to ensure a parallel anvil alignment and a long waiting time (at least 2–3 days) for the cell to relax after each pressure change, our Pb manometer showed sharp superconducting transitions of width $\Delta T_c \leqslant 0.1$ K. This indicates that pressure gradients did not exceed 4 kbar, which is not much worse than what has been reported for common liquid pressure media [6]. This is further confirmed by the similarity of our pressure phase diagram to literature data [22].

A photograph of the experimental setup is shown in Fig. 1 together with a sketch showing the arrangement. Twelve 50 μm thin electric wires were fed through 70 μm narrow grooves in the gasket to electric contacts on the sample, to a resistive heater at a short distance from the sample, to two pairs of Au-Fe(0.07%)/Chromel thermocouples in contact with the samples and to electric contacts on the Pb manometer. The sample and the wires were placed on a thin disk made of steatite and fixed with tiny drops of epoxy resin. The Au wires are simply placed onto the sample and the manometer, so that the electric contacts will be established when pressure is applied to the cell. The contacts between the thermocouple legs were made with a small drop of silver epoxy. After completion of the setup, it was covered by a second disk of steatite and some pyrophillite powder was placed to cover the wires in the grooves through the gasket for electric insulation from the top anvil.

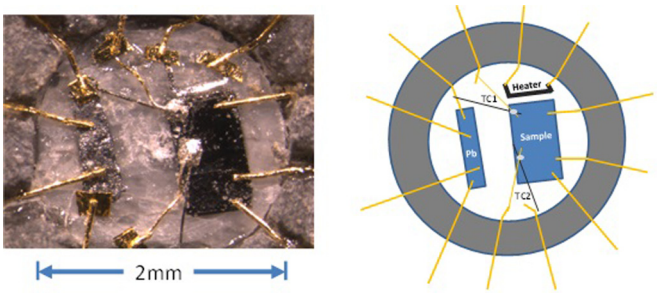

FIG. 1. Experimental configuration in the gasket (gray ring on the edge of the picture) of the Bridgman cell on top of one anvil. (Left-hand photograph, right-hand sketch.) The dark rectangle on the right is the $Ba_{0.85}K_{0.15}Fe_2As_2$ single crystal, contacted by Au leads and two thermocouples (TC1 and TC2). The light gray stripe on the left is a foil of Pb in a four-probe resistance configuration that serves as a manometer.

The electrical transport measurements were performed using a standard four-probe technique with an ac current source in combination with a lock-in technique. The specific heat was measured with an ac temperature-modulated technique at a high modulation frequency of several hundred Hz up to 1 kHz, to achieve thermal isolation of the sample [8,19,31]. The Joule-heating resistor was used to modulate periodically the temperature of the sample and a thermocouple was used to monitor the temperature modulation with help of a low-noise transformer connected to a lock-in amplifier. The thermoelectrical measurements were carried out in a similar way, but using transverse and longitudinal electric contacts on the sample to measure the Nernst and Seebeck voltages, respectively. The temperature gradient was determined by the two thermocouples. Both the Nernst effect and the Hall effect were measured for positive and negative magnetic fields applied perpendicular to the FeAs layers to eliminate spurious longitudinal voltages from an imperfect geometry of the electrodes. The Nernst effect data were measured during temperature sweeps at constant magnetic fields of ± 6 T. The Hall effect was measured at stabilized temperatures during field sweeps.

III. RESULTS

Figure 2(a) shows the resistivity of the sample at different pressures up to 5.5 GPa. At the lowest pressure of $p = 0.2$ GPa, T_c is indicated by a drop beginning at 14 K. Zero resistivity is reached at 10 K. A certain change in the slope marks the beginning of nematic and stripe-type SDW order below $\sim$120 K. The transition is more obvious in the temperature derivative of the resistivity $d\rho/dT$ [Fig. 2(b)], which displays a sharp peak at $T_{sN} = 112$ K. At higher pressure this magnetostructural transition is barely visible in the resistivity, which is likely a consequence of strain-induced broadening of the nematic transition by our quasihydrostatic conditions. However, the transition can be traced in the form of a small bump up to 3.5 GPa in the derivative [Fig. 2(b)]. The normal state resistivity above T_{sN} is continuously decreasing with increasing pressure, even above 3.5 GPa where T_c begins to decrease. At higher pressure, the onset of the resistive T_c appears to increase rapidly and saturates at 34 K, but a

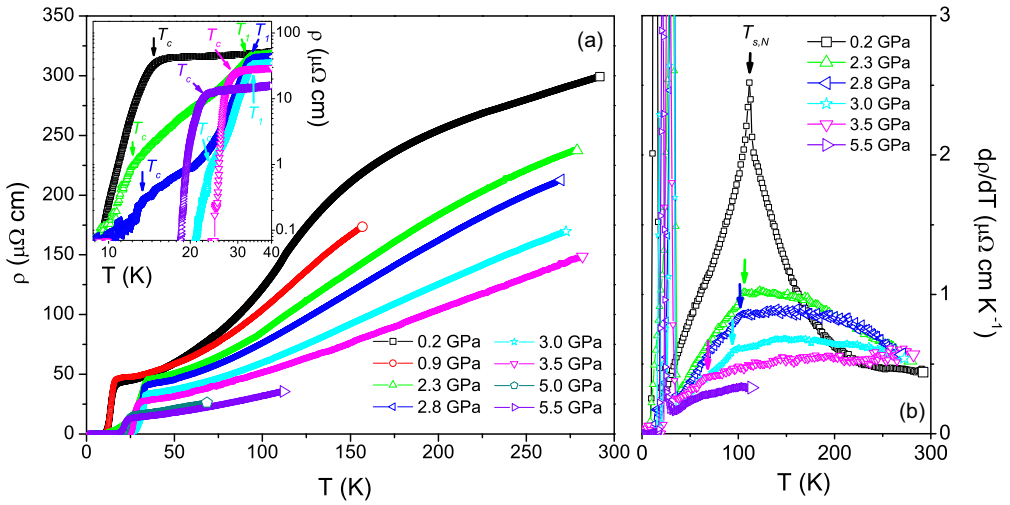

FIG. 2. (a) Resistivity of $Ba_{0.85}K_{0.15}Fe_2As_2$ under various pressures up to 5.5 GPa. The inset shows details at the superconducting transition in the low-temperature regime. (b) Temperature derivative of the resistivity. The arrows mark the onset of nematic and stripe-type SDW order.

tail of finite resistance remains down to 14 K and vanishes only at pressures of 3 GPa and higher. At higher pressure, T_c decreases, indicating that the overdoped regime is reached. At first glance, the overall behavior of $T_c(p)$ seems rather ordinary and the pressure-induced intermediate phase [22] is hidden in our experiment. The strong drop in the resistivity appears to be at first glance entirely related to superconductivity, with the T_c onset increasing up to 34 K at 3 GPa. However, the long tail of the resistive transition extending down to ∼14 K for pressures of 1–3 GPa indicates that in this pressure range superconductivity is disturbed, which could be evidence of the presence of the intermediate phase. This is more evident in the inset of Fig. 2(a), which shows the transition regime on a double logarithmic scale. In this plot, a double-step feature at T_c (which we define in the following by the steplike anomaly in the low-temperature regime) and T_1 (defined at the onset of the upper steplike anomaly) becomes obvious for the data at 2.3, 2.8, and 3 GPa. This agrees with Hassinger's observations [22], although the drop in resistivity is much more pronounced in our experiment. A certain nonhydrostatic pressure component in our pressure cell likely causes some stress in the sample, and this may be the reason for the much lower resistivity of this intermediate phase in comparison to Hassinger's data [22]. In our experiment, the intermediate phase involves filamentary superconductivity, as we will demonstrate later.

In the following experiments, we concentrate on the low-pressure range up to 3 GPa, for which we have specific heat and thermoelectric data, and investigate in detail the pressure-induced intermediate state between T_c and T_1.

Figure 3 shows the specific heat at 0.2, 2.3, and 3 GPa. A sharp BCS-type superconducting transition with $T_c = 13.7$ K is seen at 0.2 GPa (see lower right-hand inset for details). The specific heat jump occurs close to the temperature of the onset of the resistivity drop. At 2.3 and 3 GPa, T_c does not increase, but actually decreases marginally to 13.5 K and remains at this temperature at 3 GPa, and a further anomaly appears with a maximum at ∼32 K and onset at ∼34 K for both pressures. In the upper left-hand inset, we have subtracted an approximate phonon background, which shows the presence of the two distinct anomalies in this pressure range in detail. The onset of this transition anomaly coincides with the temperature where the resistance starts to drop in this pressure range. The specific heat as a bulk thermodynamic probe thus confirms that a distinct intermediate phase exists between $T_c = 13.5$ K and $T_1 = 34$ K for this pressure range, which is characterized by a small but finite resistance. The steplike shape of the anomaly at T_1 suggests that the transition is of second order, in contrast to the first-order transition that restores the C_4 rotational symmetry in $Ba_{1-x}K_xFe_2As_2$ at ambient pressure [23]. This may, however, be an artifact caused by pressure gradients.

The thermoelectric Nernst effect has been proven to be a powerful tool for understanding the phase diagram of superconductors [32–34]. While the Nernst coefficient is usually very small for ordinary metals in their normal state,

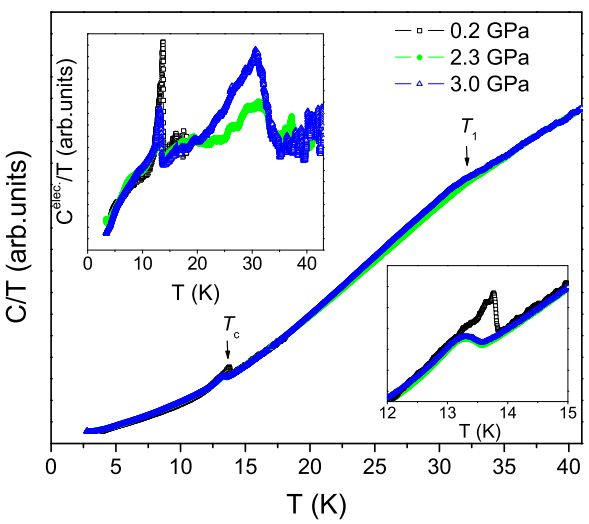

FIG. 3. Specific heat of $Ba_{0.85}K_{0.15}Fe_2As_2$ under pressures of 0.2, 2.3, and 3.0 GPa. The lower right-hand inset shows details at the superconducting transition temperature T_c. In the upper left-hand inset, an approximate phonon background has been subtracted. This clearly reveals the presence of a further anomaly at $T_1 > T_c$ in the 2.3 and 3 GPa data.

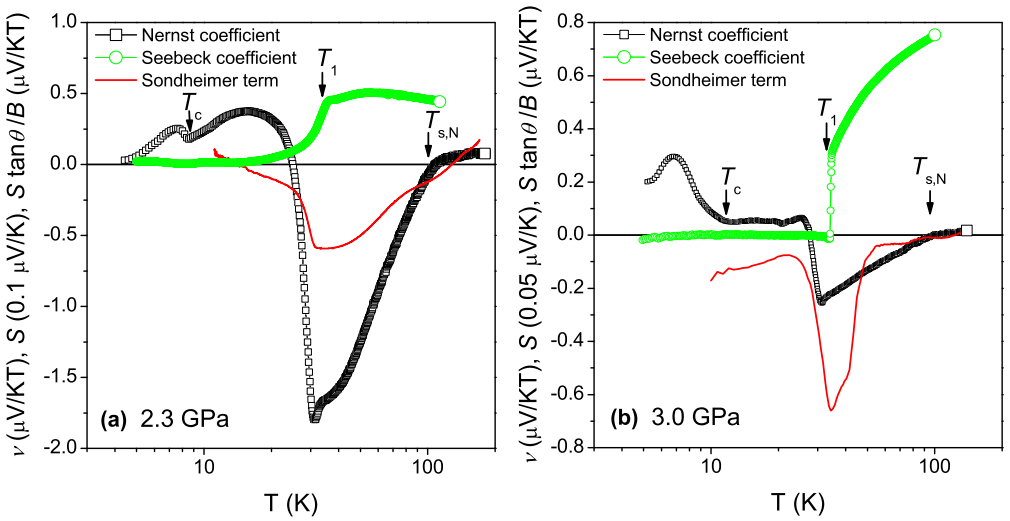

FIG. 4. Temperature dependence of the Nernst coefficient $\nu = N/B$ in a field of 6 T applied perpendicular to the FeAs layers (black open dots), the zero-field thermopower (green squares, scaled for comparison), and the Sondheimer term $S \tan\theta/B$ (red line) of $Ba_{0.85}K_{0.15}Fe_2As_2$ at pressures of (a) 2.3 GPa and (b) 3 GPa.

a large positive contribution from vortex motion results in type-II superconductors in addition to the regular normal state contribution, and has been used to monitor the presence of superconducting fluctuations above T_c [32]. In addition, the Nernst coefficient is particularly sensitive to nematic order arising from electronic correlations that spontaneously break the rotational symmetry, as observed in various cuprate and Fe-based superconductors [34]. Figure 4 shows the thermoelectric Nernst (in a 6 T field) and zero-field Seebeck coefficients measured at 2.3 and 3 GPa. The Seebeck coefficient primarily mimics the resistivity and drops at both pressures below ~34 K, presumably due to filamentary superconductivity. The Nernst coefficient shows two distinct anomalies, which we attribute to the transitions observed at T_c and T_1 in the specific heat. The fact that the anomaly at T_c appear slightly below the specific heat transition can be explained by the applied 6 T magnetic field, which typically reduces T_c in underdoped $Ba_{1-x}K_xFe_2As_2$ samples by at least 2 K [35]. A pronounced positive signal appears for both pressures below T_c, which clearly corresponds to vortex motion [32]. The data remain positive up to T_1, although the data at 2.3 and 3 GPa show a somewhat different behavior in this temperature regime. At 2.3 GPa, there is a broad positive bump between T_c and T_1. At 3 GPa, a plateau with a finite small positive value is observed in this temperature range. At T_1 the Nernst coefficient changes abruptly to a large negative signature in the form of a steep drop when the temperature is increased. Such a giant normal-state Nernst coefficient is regarded as a signature of nematic order, which is related to a symmetry-breaking Fermi surface reconstruction [34]. It has been observed previously for $LaFeAsO_{1-x}F_x$ [33] and $CaFe_{2-x}Co_xAs_2$ [36], but its magnitude is particularly large here. In the high-temperature region, the negative signal magnitude decreases gradually and crosses zero at ~90 K before it saturates at a small positive value at ~104 K, where the nematic and SDW order vanishes. The magnitude of this negative contribution is smaller at 3 GPa, which indicates that the nematic and SDW orders become suppressed rapidly at higher pressure, even though the antiferromagnetic transition appears only slightly decreased to ~94 K.

The Nernst data further confirm that a distinct intermediate phase is present between T_c and T_1. In this phase the strongly negative contribution observed in the stripe-type SDW phase is absent. Since this negative contribution is associated with the nematic order that more or less coincides with the stripe-type SDW state in $Ba_{1-x}K_xFe_2As_2$ [34], we can conclude that in this intermediate phase nematic order is suppressed and it thus shows similar characteristics to the reentrant C_4 phases observed in $Ba_{1-x}K_xFe_2As_2$ [23] and $Ba_{1-x}Na_xFe_2As_2$ [24] at ambient pressure. The vanishing of the strongly negative Nernst coefficient in the SDW phase below T_1 demonstrates that the nematic order is suppressed in this phase. Its finite positive Nernst coefficient points to the presence of mobile vortices well above the bulk superconducting transition at T_c. We can thus conclude that the intermediate phase is a reentrant C_4 phase such as the one observed at ambient pressure [23], and that it coexists in our experiment with filamentary superconductivity.

Figure 5 shows the Hall coefficient at various fixed temperatures. The magnetic field was applied perpendicular to

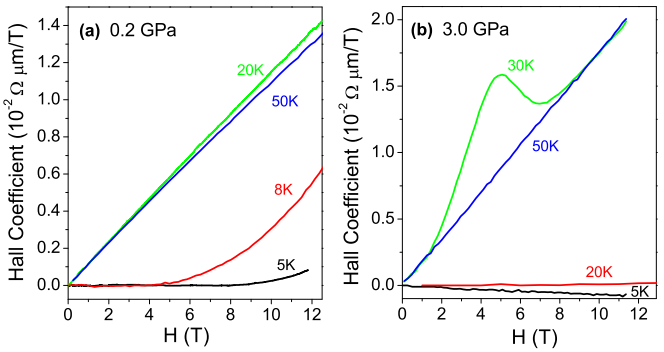

FIG. 5. Field dependence of the Hall coefficient at various temperatures at pressures of (a) 0.2 GPa and (b) 3 GPa.

the FeAs layers. Here we compare the behavior at a very low pressure of 0.2 GPa without an intermediate phase with data at 3 GPa with an intermediate phase. The Hall voltage vanishes in the entire temperature range below the bulk superconducting T_c. In the normal state it shows the expected linear field dependence. At 0.2 GPa and 5 K, the Hall voltage is zero in a field below a characteristic critical field $H_c \sim 9$ T, and then increases gradually. At 8 K, the trend is similar, but with a lower $H_c \sim 4.5$ T. At 3 GPa, the Hall coefficient almost vanishes at 20 K, and obviously H_c exceeds our available field range at this pressure. The vanishing Hall coefficient confirms that the material is still in a superconducting state from a transport point of view, in accordance with our conclusions from the Nernst coefficient and the resistivity. At 5 K, a slightly negative Hall signal is observed, presumably related to vortex flow. It is interesting that at 30 K the signal increases with a larger slope first and then goes through a maximum, and finally the linear normal-state behavior is approached. This characteristic is absent at higher temperatures. It is obviously related to the vicinity of the transition from the reentrant C_4 phase to the stripe-type SDW phase and may be a precursor of the Fermi surface reconstruction associated with the appearance of the stripe-type SDW and nematic order [37].

IV. DISCUSSION

Under the influence of a temperature gradient and an electrical field the total charge carrier current density is $J = \overleftrightarrow{\sigma} \cdot E + \overleftrightarrow{\alpha} \cdot (-\nabla T)$, where α is the Peltier coefficient tensor and σ is the conductivity tensor. The resulting transverse Nernst voltage is then

$$N = \frac{E_y}{\nabla_x T} = \frac{\alpha_{xy}\sigma_{xx} - \alpha_{xx}\sigma_{xy}}{\sigma_{xx}^2 + \sigma_{xy}^2}. \tag{1}$$

The solution of the Boltzmann equation leads to the following relationship between the electrical and the thermoelectrical conductivity tensors:

$$\bar{\alpha} = -\frac{\pi^2}{3}\frac{k_B^2 T}{e}\frac{\partial \sigma}{\partial \varepsilon}\bigg|_{\varepsilon=\varepsilon_F}. \tag{2}$$

Substitution into Eq. (1) yields

$$N = -\frac{\pi^2}{3}\frac{k_B^2 T}{e}\frac{\partial \tan\theta_H}{\partial \varepsilon}\bigg|_{\varepsilon=\varepsilon_F}. \tag{3}$$

For a single band system, the Hall angle can be expressed in terms of the cyclotron frequency and scattering time. Therefore, an alternative description of the Nernst effect is [38]

$$\nu = NB = -\frac{\pi^2}{3}\frac{k_B^2 T}{m^*}\frac{\partial \tau}{\partial \varepsilon}\bigg|_{\varepsilon=\varepsilon_F}, \tag{4}$$

where B is the magnetic field. Obviously, the Nernst signal is zero when the Hall angle is independent of energy. Taking into account Eq. (3) for the quasiparticle contribution only, it is clear that two cases lead to observable Nernst signals: a multiband structure, or energy-dependent Hall angles. The characteristic Fermi surface of Fe-based superconductors is responsible for the occurrence of charge carriers of two opposite signs [20] due to multiple bands. Therefore, it is crucial to analyze the quasiparticle contribution to the Nernst signal. To what extent the Nernst signal is unusual can be judged from the "Sondheimer cancellation" [38],

$$\nu = \left(\frac{\alpha_{xy}}{\sigma} - S\tan\theta\right)\frac{1}{B}, \tag{5}$$

where S is the Seebeck coefficient and θ the Hall angle. In an ordinary one-band metal the two terms cancel, resulting in a vanishing of the Nernst coefficient ν. To test whether the Sondheimer cancellation holds is therefore a powerful tool to reveal strongly correlated electronic states such as superconductivity, nematic order, or SDW states. The degree of violation of the Sondheimer cancellation can be tested experimentally, by comparing the measured ν with the term $S\tan\theta/B$ derived from thermopower and Hall effect data. For an ordinary metal it would be expected that ν is much smaller than $S\tan\theta/B$.

In Fig. 4 we added the Sondheimer terms to the plot of the Nernst and Seebeck coefficients to illustrate the result of the Sondheimer cancellation. At 2.3 GPa, the absolute magnitude of ν in the stripe-type SDW and nematic state is much larger than $S\tan\theta/B$. For LaFeAsO, the violation of the Sondheimer cancellation in this state has been explained by a Fermi surface reconstruction [33] with spontaneous breaking of rotational symmetry associated with the nematic order [37]. Upon comparing the magnitude of the negative Nernst signal with the parent compounds LaFeAsO [33] and $CaFe_2As_2$ [36], it becomes obvious that the absolute magnitude of the Nernst coefficient associated with the nematic order is particularly large for $Ba_{1-x}K_xFe_2As_2$ in this pressure range, especially regarding the fact that optimal pressure is almost reached.

The absolute magnitude of the negative signal in the stripe-type SDW state above T_1 is much larger than that of the positive vortex contribution in the bulk superconducting state below T_c. Therefore, the positive Nernst coefficient in the intermediate phase between T_c and T_1 cannot originate from a partial cancellation of positive and negative contributions. The negative Nernst signal of the nematic order thus vanishes below T_1 and becomes replaced by a positive weak vortex contribution of superconducting origin. The vortex signal is weaker than in the bulk superconducting state and the resistivity is finite, thus identifying a filamentary nature of superconductivity. A likely explanation is that the transition at T_1 into the reentrant C_4 phase is incomplete and some orthorhombic domains coexist with tetragonal domains in the volume. The pressure medium in our experiment is less hydrostatic compared to Hassinger's conditions [22]. It was reported that the transition from the nematic SDW phase into a reentrant C_4 phase in $Ba_{1-x}Na_xFe_2As_2$ is not always complete and some phase separation with spatially separated orthorhombic and tetragonal regions may exist [25]. This may depend significantly on the choice of pressure medium. Our data do not supply any information about the structure or magnetic order in the intermediate phase, but a likely explanation for our data is the coexistence of a reentrant C_4 phase and a C_2 minority phase on a microscopic length scale. The filamentary superconductivity could be associated either with the C_2 minority phase, or the domain boundaries between the two phases. On the other hand, the volume fraction occupied by the orthorhombic domains must be very small since the Nernst coefficient does not show

any sign of long-range nematic order in the reentrant C_4 phase.

At 3 GPa, the sample approaches optimal pressure conditions and the negative Nernst contribution in the stripe-type SDW phase is much smaller compared to the sample at 2.3 GPa. Indeed, the Nernst coefficient ν is now smaller than $S\tan\theta/B$ and thus the Sondheimer cancellation is no longer violated. This is in accordance with the expectation that the nematic order vanishes upon approaching the overdoped regime.

V. CONCLUDING REMARKS

The multitude of experimental data from different physical quantities which are rarely available under high-pressure conditions offers information about the pressure-induced phase diagram of slightly doped $Ba_{1-x}K_xFe_2As_2$. The data confirm the presence of a pressure-induced intermediate phase between the onset of bulk superconductivity and the stripe-type SDW state observed by Hassinger *et al.* [22], and extend the high-pressure phase diagram of $Ba_{1-x}K_xFe_2As_2$ to higher pressure to reveal the entire range that encloses the intermediate phase. In addition, our Nernst effect data show that the nematic order is absent in this phase, thus confirming that it represents a similar reentrant C_4 phase as observed for $Ba_{1-x}K_xFe_2As_2$ with higher K contents at ambient pressure. The data further reveal a highly complex interplay of superconductivity, SDW and nematic order. A compiled phase diagram is shown in Fig. 6. This phase is referred to as "filamentary SC+reentrant tet." In this intermediate phase, tetragonal regions likely coexist spatially separated with orthorhombic regions of vanishingly small volume fraction in which the ordinary stripe-type antiferromagnetic SDW order is preserved. This coexistence is likely responsible for the filamentary superconductivity. Note that filamentary superconductivity within the reentrant tetragonal phase is not only a consequence of pressure gradients, but is also observed in samples at ambient pressure [23]. This demonstrates the need for bulk thermodynamic data to reveal the true phase diagram of this material class. When the temperature is lowered, the entire sample goes into a bulk superconducting state in which the larger positive Nernst coefficient indicates a liquid vortex phase. At higher pressure, the intermediate state shrinks and finally disappears at 3 GPa. We added Hassinger's data [22] for a 16% K doped sample (stars) in the phase diagram shown in Fig. 6, which is in perfect agreement with our data.

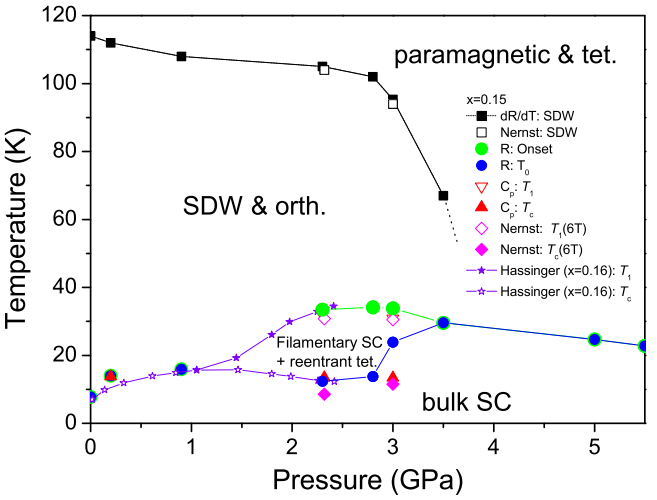

FIG. 6. Phase diagram of $Ba_{0.85}K_{0.15}Fe_2As_2$ compiled from the resistivity, specific heat, and Nernst coefficient data (tet., tetragonal; orth., orthorhombic; SDW, stripe-type antiferromagnetic spin density wave state; SC, superconducting state). The stars are data taken from Ref. [22] for $Ba_{0.84}K_{0.16}Fe_2As_2$.

The lower bulk T_c values in the pressure range of the reentrant tetragonal phase demonstrate that the reentrant C_4 phase competes particularly strongly with superconductivity under pressure. The onset of filamentary superconductivity associated with the orthorhombic minority domains can be taken as an estimation of how high T_c could be if the reentrant C_4 phase was absent. The specific heat data, which provide the bulk thermodynamic values of the transition temperatures, reveal that the bulk T_c is suppressed as much as ~20 K (from 34 K down to 13.5 K) by the reentrant tetragonal order.

ACKNOWLEDGMENTS

R.L. is grateful to D. Jaccard for sharing his extraordinary expertise in high-pressure experiments. We further thank U. Lampe for technical support. This work was supported by grants from the Research Grants Council of the Hong Kong Special Administrative Region, China (No. 603010, No. SEG_HKUST03, and No. SRFI11SC02).

[1] P. L. Alireza, Y. T. C. Ko, J. Gillett, C. M. Petrone, J. M. Cole, G. G. Lonzarich, and S. E. Sebastian, J. Phys.: Condens. Matter **21**, 012208 (2009).

[2] E. Colombier, S. L. Bud'ko, N. Ni, and P. C. Canfield, Phys. Rev. B **79**, 224518 (2009).

[3] F. Ishikawa, N. Eguchi, M. Kodama, K. Fujimaki, M. Einaga, A. Ohmura, A. Nakayama, A. Mitsuda, and Y. Yamada, Phys. Rev. B **79**, 172506 (2009).

[4] H. Fukazawa, N. Takeshita, T. Yamazaki, K. Kondo, K. Hirayama, Y. Kohori, K. Miyazawa, H. Kito, H. Eisaki, and A. Iyo, J. Phys. Soc. Jpn. **77**, 105004 (2008).

[5] A. Mani, N. Ghosh, S. Paulraj, A. Bharathi, and C. S. Sundar, Europhys. Lett. **87**, 17004 (2009).

[6] W. J. Duncan, O. P. Welzel, C. Harrison, X. F. Wang, X. H. Chen, F. M. Grosche, and P. G. Niklowitz, J. Phys.: Condens. Matter **22**, 052201 (2010).

[7] T. Yamazaki, N. Takeshita, R. Kobayashi, H. Fukazawa, Y. Kohori, K. Kihou, C.-H. Lee, H. Kito, A. Iyo, and H. Eisaki, Phys. Rev. B **81**, 224511 (2010).

[8] Y. Zheng, Y. Wang, F. Hardy, A. E. Böhmer, T. Wolf, C. Meingast, and R. Lortz, Phys. Rev. B **89**, 054514 (2014).

[9] N. Ni, M. E. Tillman, J.-Q. Yan, A. Kracher, S. T. Hannahs, S. L. Bud'ko, and P. C. Canfield, Phys. Rev. B **78**, 214515 (2008).
[10] A. S. Sefat, R. Jin, M. A. McGuire, B. C. Sales, D. J. Singh, and D. Mandrus, Phys. Rev. Lett. **101**, 117004 (2008).
[11] M. Rotter, M. Pangerl, M. Tegel, and D. Johrendt, Angew. Chem. Int. Ed. **47**, 7949 (2008).
[12] M. Rotter, M. Tegel, and D. Johrendt, Phys. Rev. Lett. **101**, 107006 (2008).
[13] S. Avci, J. M. Allred, O. Chmaissem, D. Y. Chung, S. Rosenkranz, J. A. Schlueter, H. Claus, A. Daoud-Aladine, D. D. Khalyavin, P. Manuel, A. Llobet, M. R. Suchomel, M. G. Kanatzidis, and R. Osborn, Phys. Rev. B **88**, 094510 (2013).
[14] S. Jiang, H. Xing, G. Xuan, C. Wang, Z. Ren, C. Feng, J. Dai, Z. Xu, and G. Cao, J. Phys.: Condens. Matter **21**, 382203 (2008).
[15] S. Kasahara, T. Shibauchi, K. Hashimoto, K. Ikada, S. Tonegawa, R. Okazaki, H. Shishido, H. Ikeda, H. Takeya, K. Hirata, T. Terashima, and Y. Matsuda, Phys. Rev. B **81**, 184519 (2010).
[16] S. Drotziger, P. Schweiss, K. Grube, T. Wolf, P. Adelmann, C. Meingast, and H. Löhneysen, J. Phys. Soc. Jpn. **79**, 124705 (2010).
[17] C. Meingast, F. Hardy, R. Heid, P. Adelmann, A. Böhmer, P. Burger, D. Ernst, R. Fromknecht, P. Schweiss, and T. Wolf, Phys. Rev. Lett. **108**, 177004 (2012).
[18] S. Sharma, A. Bharathi, S. Chandra, V. R. Reddy, S. Paulraj, A. T. Satya, V. S. Sastry, A. Gupta, and C. S. Sundar, Phys. Rev. B **81**, 174512 (2010).
[19] R. Lortz, A. Junod, D. Jaccard, Y. Wang, S. Tajima, and T. Masui, J. Phys.: Condens. Matter **17**, 4135 (2005).
[20] Paglione and R. L. Greene, Nat. Phys. **6**, 645 (2010).
[21] R. M. Fernandes, A. V. Chubukov, and J. Schmalian, Nat. Phys. **10**, 97 (2014).
[22] E. Hassinger, G. Gredat, F. Valade, S. R. deCotret, A. Juneau-Fecteau, J.-Ph. Reid, H. Kim, M. A. Tanatar, R. Prozorov, B. Shen, H.-H. Wen, N. Doiron-Leyraud, and L. Taillefer, Phys. Rev. B **86**, 140502(R) (2012).
[23] A. E. Böhmer, F. Hardy, L. Wang, T. Wolf, P. Schweiss, and C. Meingast, Nat. Commun. **6**, 7911 (2015).
[24] S. Avci, O. Chmaissem, J. M. Allred, S. Rosenkranz, I. Eremin, A. V. Chubukov, D. E. Bugaris, D. Y. Chung, M. G. Kanatzidis, J.-P. Castellan, J. A. Schlueter, H. Claus, D. D. Khalyavin, P. Manuel, A. Daoud-Aladine, and R. Osborn, Nat. Commun. **5**, 3845 (2014).
[25] F. Waßer, A. Schneidewind, Y. Sidis, S. Wurmehl, S. Aswartham, B. Büchner, and M. Braden, Phys. Rev. B **91**, 060505 (2015).
[26] J. M. Allred, K. M. Taddei, D. E. Bugaris, M. J. Krogstad, S. H. Lapidus, D. Y. Chung, H. Claus, M. G. Kanatzidis, D. E. Brown, J. Kang, R. M. Fernandes, I. Eremin, S. Rosenkranz, O. Chmaissem, and R. Osborn, Nat. Phys. (2016).
[27] J. Thomasson, C. Ayache, I. L. Spain, and M. Villedieu, J. Appl. Phys. **68**, 5933 (1990).
[28] The pressure calibration for Pb-manometers from Ref. [27] was recently confirmed up to 10 GPa by S. Deemyad [29], under optimal hydrostatic conditions with ^{4}He as a pressure-transmitting medium, in contrast to the data by Bireckhoven *et al.* [30], showing deviations in the pressure range below 10 GPa.
[29] S. Deemyad, Ph.D. thesis, Washington University, St. Louis, 2004.
[30] B. Bireckhoven and J. Wittig, J. Phys. E **21**, 841 (1977).
[31] Y. Zheng, Y. Wang, B. Lv, C. W. Chu, and R. Lortz, New J. Phys. **14**, 053034 (2012).
[32] Y. Wang, L. Li, and N. P. Ong, Phys. Rev. B **73**, 024510 (2006).
[33] A. Kondrat, G. Behr, B. Büchner, and C. Hess, Phys. Rev. B **83**, 092507 (2011).
[34] C. Hess, in *New Materials for Thermoelectrics: Theory and Experiment*, *Proceedings of NATO Advanced Research Workshop, Hvar, Croatia, September 19–25, 2011*, edited by V. Zlatic and A. Hewson, NATO Science for Peace and Security Series B: Physics and Biophysics (Springer, Dordrecht, 2013), p. 169.
[35] J. Hou, P. Burger, H. K. Mak, F. Hardy, T. Wolf, C. Meingast, and R. Lortz, Phys. Rev. B **92**, 064502, (2015).
[36] M. Matusiak, Z. Bukowski, and J. Karpinski, Phys. Rev. B **81**, 020510(R) (2010).
[37] A. Hackl and M. Vojta, Phys. Rev. B **80**, 220514(R) (2009).
[38] E. H. Sondheimer, Proc. R. Soc. London, Ser. A **193**, 484 (1948).